



# A biophysical model of vertebrate olfactory epithelium and bulb exhibiting gap junction dependent odor-evoked spatiotemporal patterns of activity

Fábio M. Simões-de-Souza<sup>a,\*</sup>, Antônio C. Roque<sup>b</sup>

<sup>a</sup> *Departamento de Psicologia e Educação, Setor de Psicobiologia, Faculdade de Filosofia Ciências e Letras de Ribeirão Preto, Universidade de São Paulo, Ribeirão Preto, Av. Bandeirantes 3900, 14040-901 São Paulo, Brazil*

<sup>b</sup> *Departamento de Física e Matemática, Faculdade de Filosofia Ciências e Letras de Ribeirão Preto, Universidade de São Paulo, Ribeirão Preto, São Paulo, Brazil*

Received 23 April 2003; received in revised form 23 April 2003; accepted 19 August 2003

## Abstract

This work describes a biophysical model of the initial stages of vertebrate olfactory system containing structures representing the olfactory epithelium and bulb. Its main novelty is the introduction of gap junctions connecting neurons both in the epithelium and bulb, and of biologically detailed dendrodendritic synapses between granule and mitral cells in the bulb. The model was used to simulate the effect of an odor presentation on the neural activity pattern in the epithelium and bulb. During the time for which an odor is presented with a constant concentration, there are spatiotemporal patterns in the epithelium and bulb generated by the couplings due to the gap junctions and/or dendrodendritic synapses. A study varying the strength of the gap junction coupling shows that the spatiotemporal patterns, both in the epithelium and bulb, are dependent of the coupling strength. It is also shown that the olfactory bulb's spatiotemporal pattern depends on the existence of the dendrodendritic connections between mitral and granule cells. If these spatiotemporal patterns really exist in the early processing stages of the olfactory system they may be used for odor coding and the gap junctions and dendrodendritic synapses might have a role on it.

© 2003 Elsevier Ireland Ltd. All rights reserved.

*Keywords:* Olfactory system; Gap junctions; Dendrodendritic synapses; Spatiotemporal coding; Computational modeling

## 1. Introduction

One of the leading hypotheses for odorant coding in the olfactory system is that identity and concentration are represented by spatiotemporal patterns of activity distributed across populations of neurons at each level of the olfactory pathway (Pearce, 1997; Êrdi et al.,

1998; White and Kauer, 1999, 2001; Friedrich and Stopfer, 2001; Laurent et al., 2001; Friedrich, 2002; Spors and Grinvald, 2002). In order to verify this hypothesis, in parallel with the development and/or improvement of experimental techniques to register and analyze simultaneously the activity of large neural populations throughout the olfactory system, it also is important to construct large-scale computational models of the olfactory system that can generate spatiotemporal activity patterns to be used as tools for investigating possible coding schemes supported by them.

\* Corresponding author. Tel.: +55-16-6023859; fax: +55-16-6339949.

*E-mail address:* [fabioms@neuron.ffclrp.usp.br](mailto:fabioms@neuron.ffclrp.usp.br) (F.M. Simões-de-Souza).

Olfactory processing starts at the level of olfactory sensory neurons (OSNs) in the olfactory epithelium (Trotier and MacLeod, 1983; Morrison and Constantino, 1990; Schild and Restrepo, 1998). Each OSN generally expresses only one type of odorant transmembrane receptor, and all neurons expressing a given receptor are randomly organized inside a so-called zone of the olfactory epithelium (Ressler et al., 1993; Vassar et al., 1993), forming what can be regarded as a mosaic arrangement comprising several different neuronal populations (Mombaerts et al., 1996). This mosaic arrangement probably changes during the lifetime of an individual because of the processes of degeneration and regeneration of OSNs, which occur every 30–45 days for the entire life (Graziadei and Graziadei, 1979). Recent evidence in favor of this mosaic arrangement has been provided by Ma and Shepherd (2000), who demonstrated in detail a functional mosaic organization in the olfactory epithelium with the existence of tight clusters of OSNs and large densities of dispersed OSNs that respond to the same odor intermingled with OSNs responding to other odors.

Another recent discovery is that the gap junction subunit connexin 43 is strongly expressed in ventrolateral areas of the olfactory epithelium by mature OSNs (Zhang et al., 2000). This raises the possibility that gap junctions might exist and have a functional role on information processing in the olfactory epithelium at least in ventrolateral regions. But the role of electrotonic coupling at the level of OSNs is not yet understood (Zhang et al., 2000).

The second level of olfactory information processing takes place in and around the glomeruli of the olfactory bulb, where the OSNs make excitatory synapses with the dendrites of mitral and tufted cells, and with periglomerular cells (Morri et al., 1998; McQuiston and Katz, 2001). Although the axons of OSNs expressing the same receptor converge at fixed sites in only a few of the bulb's glomeruli forming a stereotyped sensory map in the bulb (Ressler et al., 1994; Vassar et al., 1994; Mombaerts, 1996; Mombaerts et al., 1996), each single receptor can recognize multiple odorants and a single odorant can be recognized by multiple receptors (Malnic et al., 1999). Therefore, different combinations of receptors and consequently of overlapping activity patterns involving multiple glomeruli may be recruited to recognize each different odorant (Malnic et al., 1999). Several

works have shown these broadly tuned responses of single OSNs and mitral/tufted cells to different odors (Gesteland et al., 1965; Getchell, 1974; Duchamp et al., 1974; Revial et al., 1978; Wellis et al., 1989; Morri et al., 1992; Firestein et al., 1993; Sato et al., 1994; Hirono et al., 1994; Bozza and Kauer, 1998; Duchamp-Viret et al., 1999; Malnic et al., 1999). Also, several imaging techniques (for reviews see, e.g. Kauer and White, 2001; Korsching, 2002) as voltage sensitive dyes (Cinelli et al., 1995; Friedrich and Korsching, 1998; Lam et al., 2000; Spors and Grinvald, 2002), calcium imaging (Bozza and Kauer, 1998; Malnic et al., 1999; Ma and Shepherd, 2000; Wachowiak and Cohen, 2001; Fried et al., 2002; Wachowiak et al., 2002) and intrinsic signals (Rubin and Katz, 1999; Uchida et al., 2000; Belluscio and Katz, 2001; Bozza and Mombaerts, 2001; Meister and Bonhoeffer, 2001) have shown different odor-evoked activity maps in the olfactory bulb.

The third level of representation occurs at the bulbar layers containing mitral and tufted cells (Hamilton and Kauer, 1989; Heyward et al., 2001), and granule cells (Woolf et al., 1991). At this level, synaptic interactions between mitral and granule cells include both inhibitory and excitatory synapses (Yokoi et al., 1995; Schoppa et al., 1998; Isaacson, 1999; Friedman and Strowbridge, 2000; Halabisky et al., 2000; Didier et al., 2001; Isaacson, 2001; Urban and Sakmann, 2002), which may play a role on the synchronized oscillatory discharges of the mitral/tufted cells (Desmaisons et al., 1999; Isaacson, 1999; Kashiwadani et al., 1999; Schoppa and Westbrook, 2001; Urban and Sakmann, 2002). Here, glutamate release from mitral dendrites excites granule cell spines, which, in turn, produce a recurrent inhibition through the releasing of inhibitory  $\gamma$ -aminobutyric acid (GABA) back onto mitral cell dendrites (Yokoi et al., 1995; Schoppa et al., 1998; Halabisky et al., 2000; Isaacson, 2001; Urban and Sakmann, 2002; Desmaisons et al., 1999; Kashiwadani et al., 1999; Schoppa and Westbrook, 2001). Recently, it has also been shown, the existence of glutamate autoreceptors in the mitral cell dendrites (Isaacson, 1999; Friedman and Strowbridge, 2000; Didier et al., 2001; Urban and Sakmann, 2002) and glutamate releasing from some granule cells (Didier et al., 2001), which suggest a process of recurrent excitation and self-excitation of the mitral cells.

Gap junctions also have been found between granule cell perikarya (Reyher et al., 1991), suggesting that there is a significant, low-resistance electrical transmission between aggregated granule cells. It was also reported that gap junctions exist between granule cell dendrites and proximal dendrites of mitral and tufted cells, thus forming dendrodendritic junctions (Reyher et al., 1991).

To investigate the possible effects of gap junction connections both at the epithelium and bulb levels, we constructed a biologically detailed model of pieces of the olfactory epithelium and olfactory bulb, with gap junctions in the two structures, and used it to study the spatiotemporal responses of these systems during odor stimulation under different situations regarding the gap junction coupling strength. We also considered two different scenarios for these studies, one in which the mitral and granule cells in the bulb are connected by dendrodendritic synapses, and one in which they are not.

## 2. The model

A biophysical model of the olfactory epithelium was built containing 2500 identical olfactory sensory neuron models (OSNMs) distributed in a  $50 \times 50$  grid. Each OSNM is composed of four compartments, namely cilium, dendritic knob, dendrite and cellular body (Simões-de-Souza and Roque, 2002). Cilium is a biochemical compartment and incorporates the molecular pathways involved in odor transduction (Menini, 1999; Zufall and Leinders-Zufall, 2000). Dendrite is a passive compartment and the dendritic knob has  $\text{Ca}^{2+}$ -dependent chloride channels (Hallani et al., 1998). Cellular body has sodium, potassium and calcium channels that produce action potentials (Schild and Restrepo, 1998). A pool of molecular odors, which increase the  $\text{Ca}^{2+}$  intracellular concentration by opening cAMP-activated cyclic nucleotide-gated channels (CNG channels), provides input to the model cell. This leads to opening of  $\text{Ca}^{2+}$ -dependent chloride channels, causing membrane depolarization and generating action potentials at the soma. The depolarization effect generated by the CNG channels was not explicitly represented in the model. It was simulated by an increase in the maximum conductance of the  $\text{Ca}^{2+}$ -dependent chloride channels.

This simplification can be justified because the  $\text{Ca}^{2+}$ -dependent chloride channels are responsible by as much as 85% of the receptor current in mammalian OSNs (Lowe and Gold, 1993; Kurahashi and Yau, 1994).

The OSNMs are connected among themselves exclusively via gap junctions, modeled as constant passive resistances (Traub et al., 1999), and each OSNM is connected to its first eight neighbors in the grid. There is a more complex model of a dynamic voltage and time-dependent gap junction made by connexin 43 (Henriquez et al., 2001), however a constant resistance in general may be a good model to simulate gap junctions, and no important difference was found between the dynamic gap junction model and the constant gap junction model regarding the shape and conduction velocity of propagating action potentials (Henriquez et al., 2001). For poorly coupled systems, the dynamic gap junction model shows significant differences in relation to the constant model (Henriquez et al., 2001), however this is not the case of the present work.

To study the effect of the gap junction coupling strength, some values of the fixed resistance of the simulated gap junction were considered within a range of physiologically relevant values, namely: 75, 300, 600, and 1200  $\text{M}\Omega$ . The case with gap junctions blocked also was considered.

The constructed epithelium model can respond to eight different odors simultaneously. The model's spatial distribution of odor sensitivity was an attempt to reproduce the experimental results of Ma and Shepherd (2000). In their paper, Ma and Shepherd mapped different areas of the olfactory epithelium and were able to identify the spatial position of the cells with the corresponding odor or odors (some cells were found to respond to more than one odor) that excited each one of them. We made a composition using three of these areas—shown in Figs. 4, 5 and 6 of Ma and Shepherd's paper (2000)—into a single square area, which was superimposed over the left half of the  $50 \times 50$  epithelium model grid. An identical replica of this composition was superimposed over the right half of the grid. In this way, each one of Ma and Shepherd's cells was assigned to one node on the left side and one node on the right side of the  $50 \times 50$  grid (see Fig. 1). Since the grid with 2500 cells has a number of 162 odor-sensitive cells, which corresponds to only 6.48% of the total, all the other 2338 OSNMs in the grid (93.52% of the

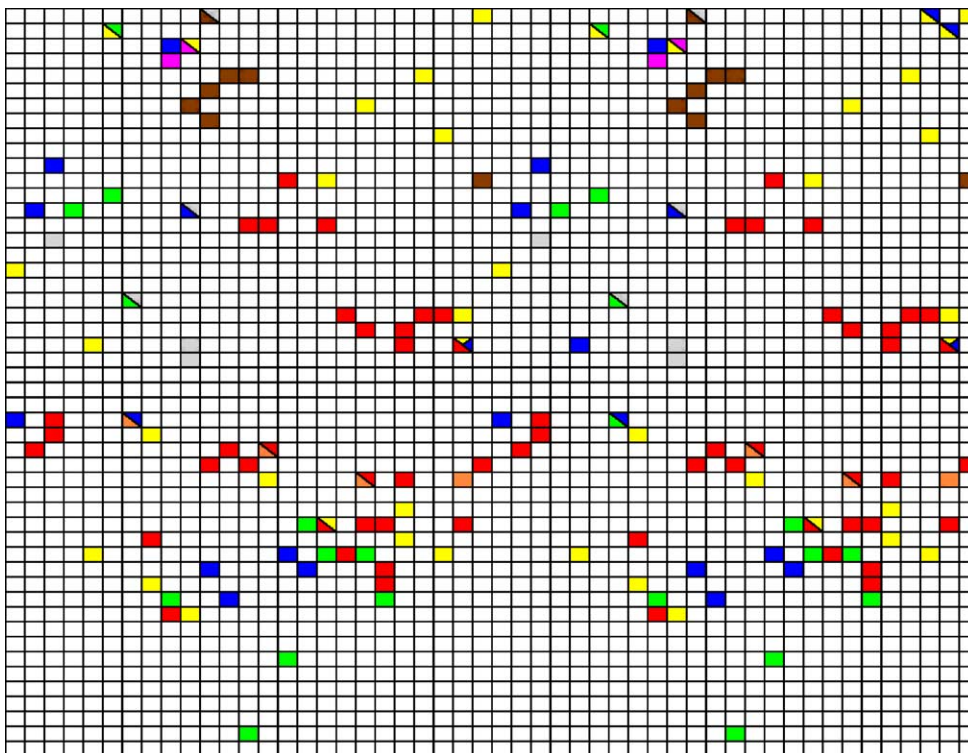


Fig. 1. Schematic representation of the  $50 \times 50$  epithelium model grid with 2500 cells, which can respond to eight different odors, namely *n*-amyl acetate (red), acetophenone (yellow), cineole (green), 3-heptanone (blue), octanol (pink), octanal (brown), octanoic acid (gray) and benzaldehyde (orange). The white color represents the cells that do not respond to any of the eight odors. Each little square in the grid corresponds to a receptor cell and the colors inside it represent the different odors to which the cell can respond.

total) were considered as non-responsive to any of the eight odors considered. They only could be excited via the gap junctions.

The OSNM response depends only on the variable “odor concentration,” without taking into consideration a particular odor’s molecular structure. Therefore, the assignment of an odor or odors to a given OSNM in the grid was made by hand to implement the distribution explained in Fig. 1. Although the chemical formula of an odor has no meaning in our simulations, the names of the eight odors used by Ma and Shepherd were kept to facilitate their identification. In this way, the 162 odor-sensitive OSNMs were distributed in the following way: 60 cells responded to *n*-amyl acetate (2.4% of the total), 44 to acetophenone (1.76%), 22 to cineole (0.88%), 26 to 3-heptanone (1.04%), 4 to octanol (0.16%), 14 to octanal (0.56%), 12 to octanoic acid (0.48%) and 8 to benzaldehyde (0.32%). Notice

that some cells can respond to two or three different odors.

The olfactory bulb model was constructed with 64 identical mitral neuron models (MNM) arranged in an  $8 \times 8$  grid and 100 identical granule neuron models (GNM) arranged in a  $10 \times 10$  grid. The MNM and GNM were constructed as simplifications of Bhalla and Bower’s (1993) detailed single-neuron models. The MNM is composed of seven compartments: tuft, soma, primary dendrite and four secondary dendrites. The GNM is composed of 12 compartments: soma, deep dendrite, trunk and peripheral dendrite with four spines of one neck and one head (the details about the parameters used to model the cells can be found in the Appendix A).

Each MNM is connected to four adjacent GNMs through dendrodendritic synapses between the secondary dendrites and the spines (Morri et al., 1998),

forming a circuit of self-inhibition and lateral-inhibition. These dendrodendritic synapses were simulated according to a model proposed by Brennan and Keverne (1997). Depolarization in a mitral cell dendrite increases the release of glutamate, which opens *N*-methyl-D-aspartate (NMDA) and  $\alpha$ -amino-3-hydroxy-5-methyl-4-isoxazolepropionate (AMPA) receptor channels in the granule cells dendritic spines. The calcium that flows mainly through NMDA receptor channels increases the release of GABA, which opens GABA<sub>A</sub> receptor channels in the mitral cell dendrites (Halabisky et al., 2000). The AMPA and NMDA synaptic channel models are based in the model of Zador et al. (1990), and the GNM dendritic spines and calcium diffusion mechanisms are based in the model of De Schutter and Smolen (1998). The recurrent excitation and self-excitation circuits involving the mitral cells glutamate autoreceptors were not simulated in the present work. Besides these dendrodendritic synapses, the MNM secondary dendrites were connected by gap junctions to the GNM dendritic spines (Reyher et al., 1991). Also, the GNMs were connected among themselves via gap junctions linking their somata (Reyher et al., 1991).

Since the epithelium model can respond to eight different odor types the olfactory bulb model was divided into eight glomeruli, each one composed of eight mitral cell tufts. Each modeled OSN which responds to the same odor converges one excitatory axon to all mitral cells that constitute a single specific glomerulus in the olfactory bulb. The OSNMs that can respond to two or three different odors also converge their axons to only one glomerulus in the model bulb, which was determined by a random choice from the two or three possible convergent glomeruli. This was necessary because Ma and Shepherd (2000) give only the positions of the OSNs that respond to a given odor, and not the odorant receptor type expressed by them. Notice that this connection pattern produces some degree of glomeruli overlap, in which a glomerulus can respond to multiple odorants and one odorant may be recognized by multiple glomeruli. The OSNMs that are non-responsive to any of the eight simulated odors do not converge axons to glomeruli in the bulb.

The works of Belluscio and Katz (2001) and Meister and Bonhoeffer (2001) have shown that there exists an antero-posterior topographic distribution of glomeruli

that respond to aliphatic odors in the bulb, forming an odotopic map, so that the larger the carbon chain of the aliphatic odor molecule, the more anterior is its position in the bulb. To model this situation, the axons of the OSNMs responsive to non-aliphatic odors (acetophenone, benzaldehyde, and cineole) converge to glomeruli in the right side of the bulb, considered to be the anterior region. The axons of the aliphatic odor-responsive OSNMs (the other five odors) converge to the glomeruli that were left in a way that respected the topographic dependence with the carbon number in the chain, from the antero side (more carbons) to the posterior side (less carbons). Of course, this simulated antero-posterior topographic map is an oversimplification and do not intend to reproduce all the complexity of the real system.

The model's equations were implemented using the GENESIS neural simulator (Bower and Beeman, 1998) running under the Linux operating system on a Pentium IV PC. The results of the simulations were further processed and the graphs were generated using MATLAB<sup>®</sup> and Microsoft Excel<sup>®</sup>.

### 3. Results

To investigate the effects of the gap junctions and dendrodendritic synapses in the model, we performed several simulations in which the experimental protocol was identical, consisting of the presentation of odor acetophenone to the system. The difference from one simulation to the other was in the strength of the gap junction coupling and in the existence or not of dendrodendritic synapses in the bulb. The following cases were considered: (1) all gap junctions in the epithelium and bulb and dendrodendritic synapses in the bulb blocked; (2) gap junctions of varying strength both in the epithelium and bulb (the same strength was used for the two areas), and dendrodendritic synapses blocked in the bulb; (3) gap junctions of varying strength both in the epithelium and bulb and dendrodendritic synapses in the bulb; (4) gap junctions of a given strength (300 M $\Omega$ ) in the epithelium, and gap junctions and dendrodendritic synapses blocked in the bulb; (5) gap junctions of 300 M $\Omega$  in the epithelium and dendrodendritic synapses in the bulb but gap junctions blocked in the bulb; (6) gap junctions in the epithelium and dendrodendritic synapses in the bulb

blocked but gap junctions of  $300\text{ M}\Omega$  in the bulb; and (7) gap junctions in the epithelium blocked but gap junctions of  $300\text{ M}\Omega$  and dendrodendritic synapses in the bulb.

The objective of the latter four cases was to assess the cases in which the epithelium does not have gap junctions but the bulb has, and vice versa, in the two scenarios of dendrodendritic synapses in the bulb (with them or without them), and not to investigate the role of the gap junction coupling strength as in the former ones. This is the reason why we used only a single gap junction coupling strength. The results obtained in these studies are described below.

The first rows of Figs. 2–4 show the responses of the olfactory epithelium, mitral cell layer and granule cell layer at three different instants in time for Case 1, with all gap junctions and dendrodendritic synapses blocked. In the epithelium, only those OSNMs that respond to the odor acetophenone are activated. They can be seen as the red dots in the first row of Fig. 2. In the mitral layer, the first MNMs that become depolarized are the eight ones that belong to the glomerulus to which the OSNMs that respond exclusively to acetophenone send their axons (the red rectangle in the 3 s column of the first row of Fig. 3). Let us call this the ‘acetophenone glomerulus.’ However, since there are some OSNMs that respond to acetophenone and other odors (as can be seen in Fig. 1) there are some MNMs outside of this glomerulus that become active over time. This can be seen at the columns for 5 and 7 s in the first row of Fig. 3. Notice, though, that the eight MNMs in the acetophenone glomerulus remain active during the entire course of the simulation. On the other hand, the response of the granule cell layer with gap junctions and dendrodendritic synapses blocked does not change over time (all cells remain at the same low activity level indicated by the green color in the first row of Fig. 4). This is due to the isolation of these cells from the mitral cell layer and from each other in this case.

The remaining rows of Figs. 2–4 are relative to Case 2, i.e. with gap junctions both in the epithelium and bulb and dendrodendritic synapses blocked in the bulb. Each row of these figures corresponds to a given value of gap junction coupling strength (the same for both the epithelium and bulb). In Fig. 2, the second row shows the epithelium response for a weak gap junction coupling ( $R_{\text{gap}} = 1200\text{ M}\Omega$ ). Notice the ap-

pearance of a time varying activity pattern involving more neurons than those which respond exclusively to the odor acetophenone. The spatial patterns for times 5 and 7 s look like thin spiral filaments. The third and fourth rows of Fig. 2 show the epithelium responses for gap junction coupling strengths of 600 and  $300\text{ M}\Omega$ , respectively. In both of these cases the activity filaments become much wider, occupying most of the epithelium area, and interact during the time span of the simulations leading to wave annihilation and wave break. The final row of Fig. 2 shows what happens when the gap junction coupling is too strong ( $R_{\text{gap}} = 75\text{ M}\Omega$ ). The complex activity pattern across the epithelium disappears and only some focused activity areas can be observed. Rows 2–5 of Figs. 3 and 4 show the corresponding responses of the mitral and granule cell layers. In the mitral cell layer with weak gap junction coupling (second row of Fig. 3), only the MNMs in the acetophenone glomerulus are active 3 s after the odor presentation but in the subsequent times other MNMs become depolarized and the initial ‘single glomerulus’ odor representation disappears. The odor representation at the mitral cell layer becomes distributed. Notice that in the subsequent times none of the MNMs in the acetophenone glomerulus are active. This phenomenon is even more pronounced for the ‘intermediate gap’ junction coupling values of 600 and  $300\text{ M}\Omega$ . In these cases the odor elicits a time varying spatial pattern in the mitral layer consisting of only a relatively small number of active MNMs at each instant of time scattered over the layer. When the gap junction coupling is too strong the spatial pattern does not change with time in the mitral layer. It consists of a pattern in which most of the cells are in resting state and only a few in each one of the glomeruli are depolarized. This may occur because of current leakages from the cells through their low resistance gap junction connections, which prevent them from reaching spike threshold. In the granule cell layer, the spatiotemporal activity patterns indicate that areas of strong activity appear around the corresponding active areas in the mitral layer. In particular, one can observe the appearance of rings of four active GNMs surrounding a corresponding cell in the mitral layer.

The responses of the mitral and granule cell layers for Case 3, with gap junction coupling both in the epithelium and bulb and dendrodendritic synapses in the bulb are shown in Figs. 5 and 6, respectively.

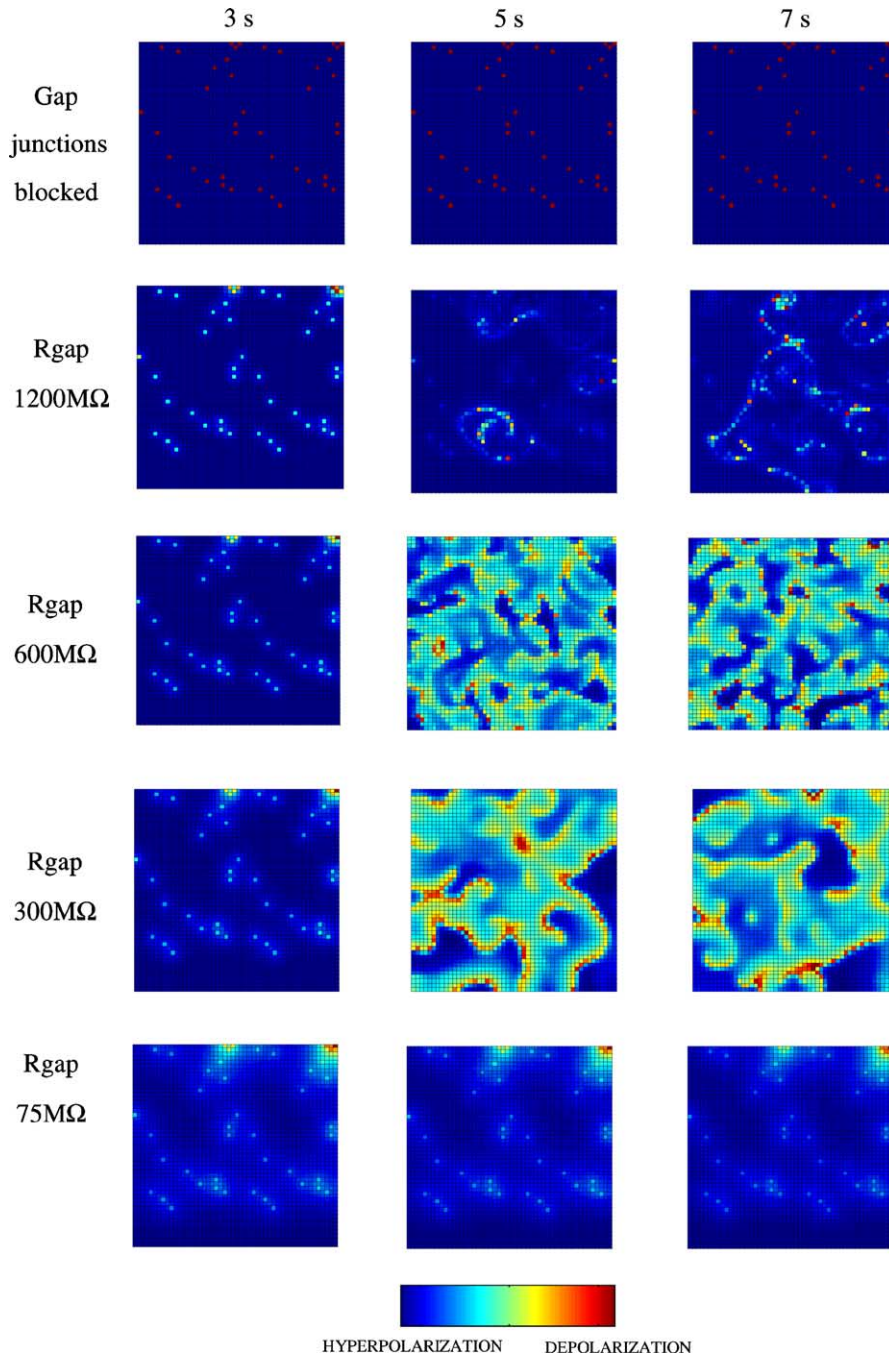


Fig. 2. Instantaneous voltage maps of the olfactory epithelium model at times 3 s (left column), 5 s (middle column) and 7 s (right column) after the presentation of  $300\mu M$  of the odor acetophenone. Each row corresponds to a given value of gap junction resistance, namely gap junctions blocked,  $1200$ ,  $600$ ,  $300$ , and  $75M\Omega$ . Each voltage map represents the epithelium grid. A color-coding scheme was used to indicate the cell's voltage value at the soma (in Volts). Hot colors represent depolarizing voltages, while cool colors represent voltages near the cell's resting potential.

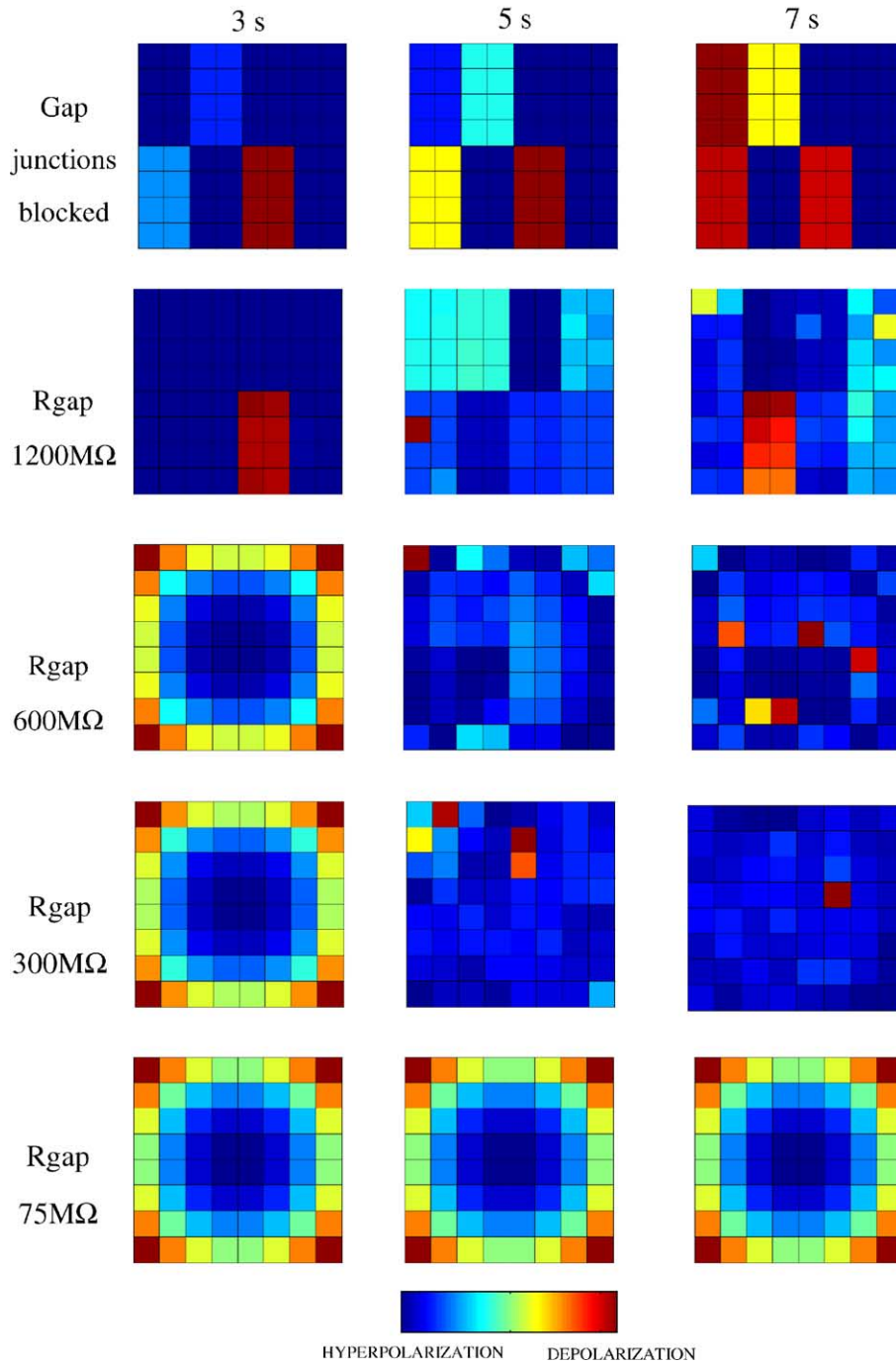


Fig. 3. Activity maps in the mitral cell layer of the model olfactory bulb for the instants 3 s (left column), 5 s (middle column) and 7 s (right column) after the presentation of  $300 \mu\text{M}$  of the odor acetophenone, for the case with gap junctions blocked or of varying strength both in the olfactory epithelium and bulb and dendrodendritic synapses blocked in the olfactory bulb. The gap junction coupling strengths are shown to the left of the rows in the figure. The color code used is the same of Fig. 2.

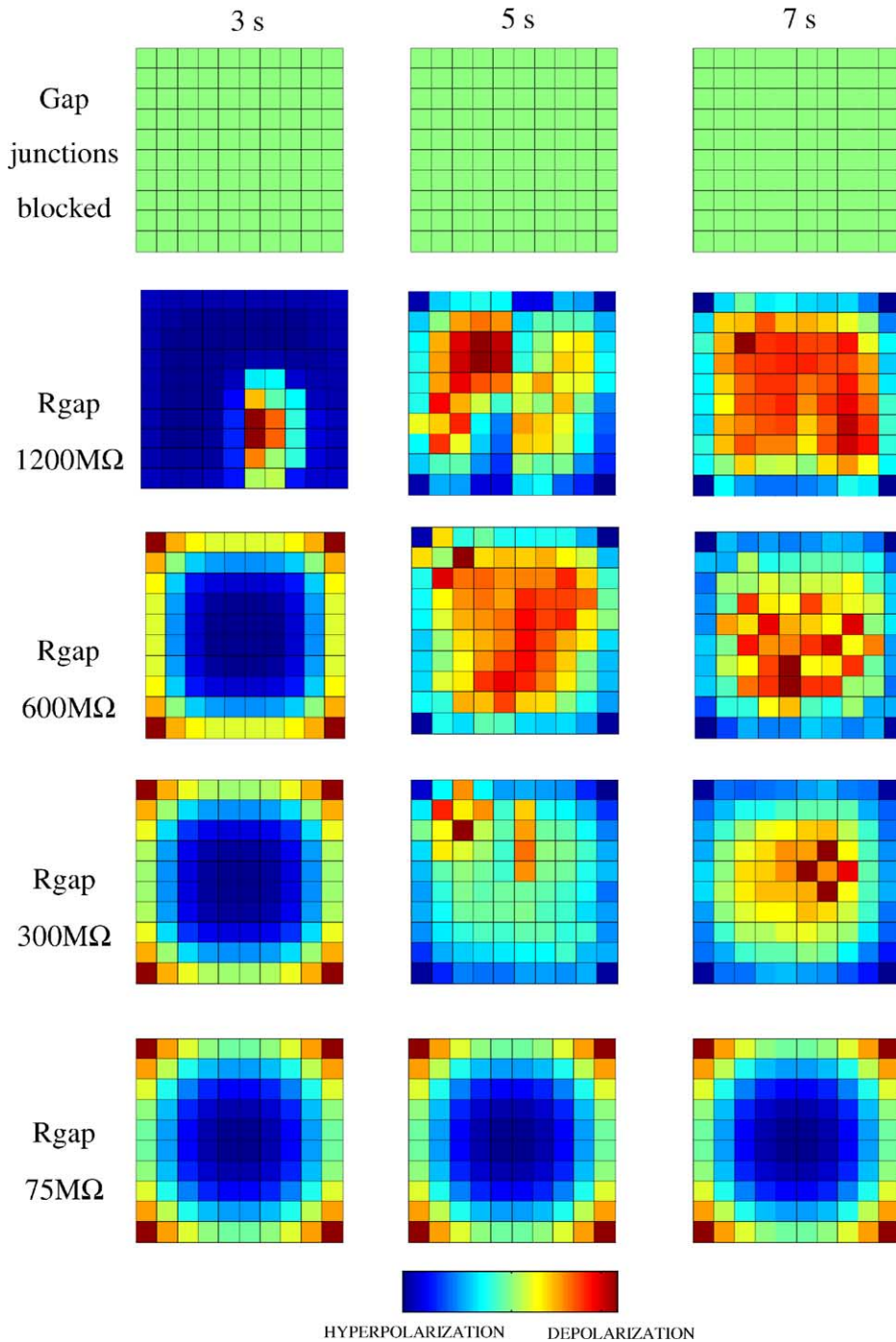


Fig. 4. Activity maps in the granule cell layer of the model olfactory bulb for the instants 3 s (left column), 5 s (middle column) and 7 s (right column) after the presentation of 300  $\mu$ M of the odor acetophenone, for the case with gap junctions blocked or of varying strength both in the olfactory epithelium and bulb and dendrodendritic synapses blocked in the olfactory bulb. The gap junction coupling strengths are shown to the left of the rows in the figure. The color code used is the same of Fig. 2.

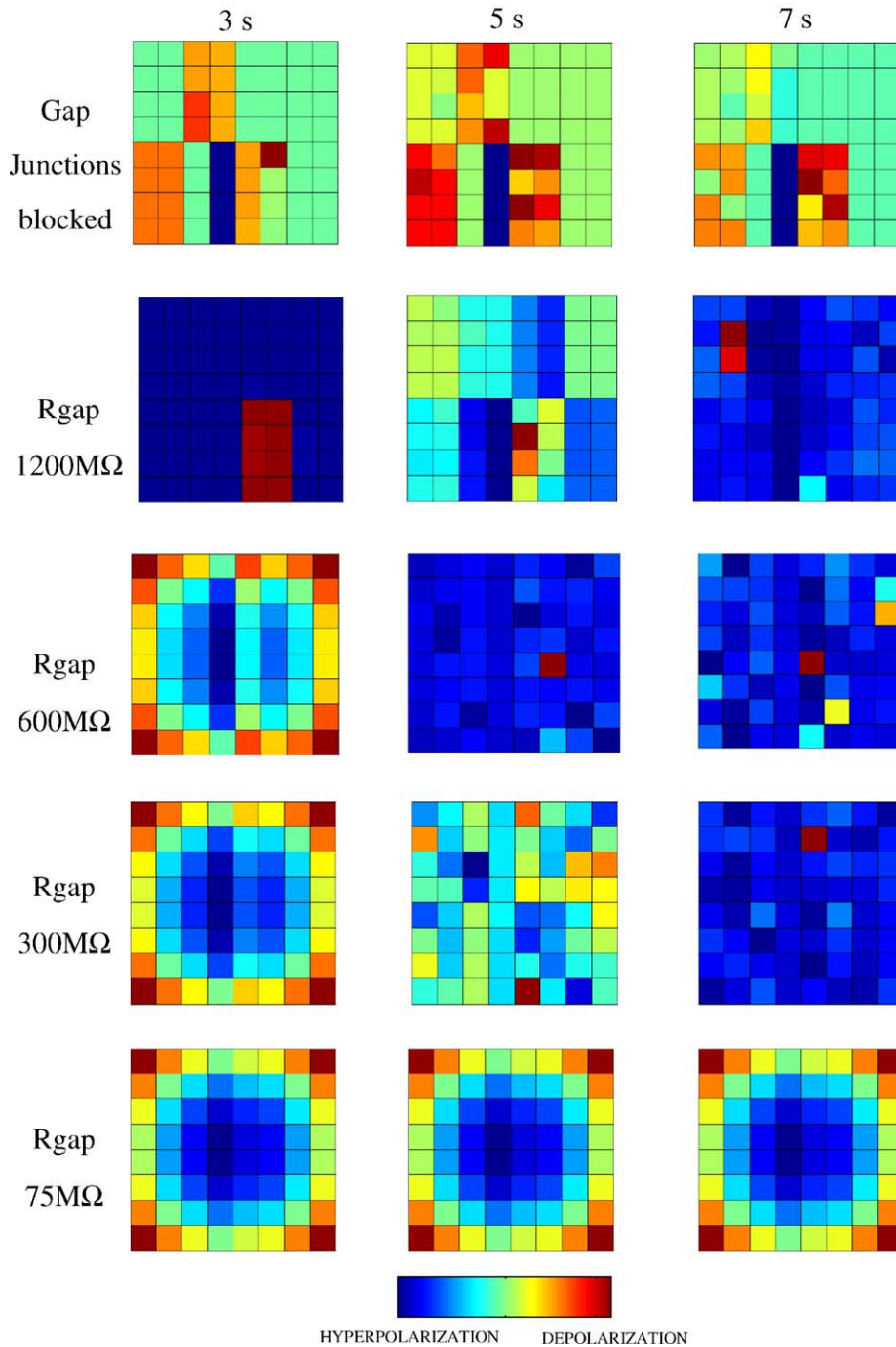


Fig. 5. Activity maps in the mitral cell layer of the model olfactory bulb for the instants 3 s (left column), 5 s (middle column) and 7 s (right column) after the presentation of 300  $\mu\text{M}$  of the odor acetophenone, for the case with gap junctions blocked or of varying strength both in the olfactory epithelium and bulb and dendrodendritic synapses in the olfactory bulb. The gap junction coupling strengths are shown to the left of the rows in the figure. The color code used is the same of Fig. 2.

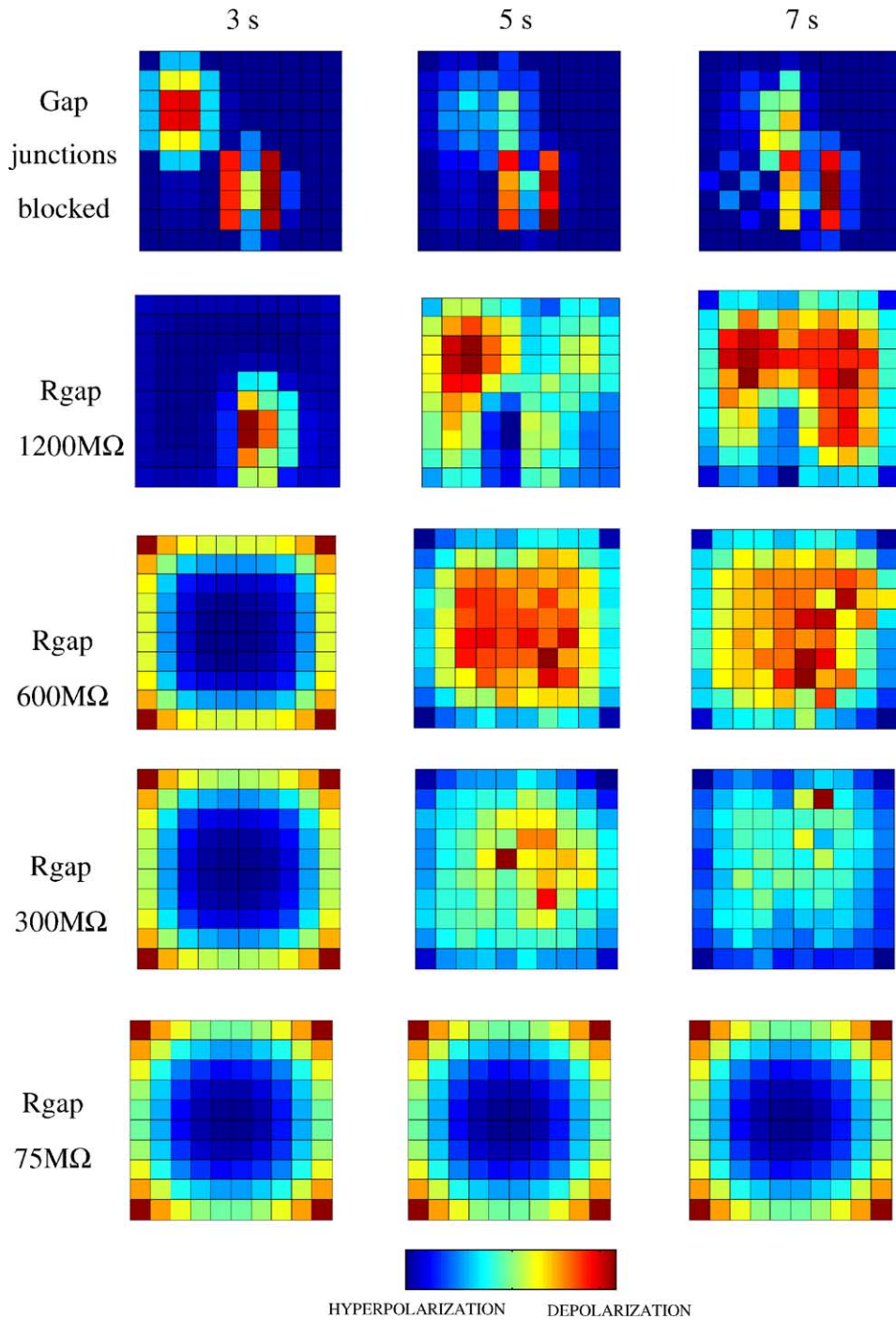


Fig. 6. Activity maps in the granule cell layer of the model olfactory bulb for the instants 3 s (left column), 5 s (middle column) and 7 s (right column) after the presentation of 300  $\mu\text{M}$  of the odor acetophenone, for the case with gap junctions blocked or of varying strength both in the olfactory epithelium and bulb and dendrodendritic synapses in the olfactory bulb. The gap junction coupling strengths are shown to the left of the rows in the figure. The color code used is the same of Fig. 2.

The first rows of Figs. 5 and 6 show what happens when there are no gap junctions in the model and the mitral and granule cells in the bulb are connected exclusively by dendrodendritic synapses. In the

mitral cell layer (Fig. 5, first row), the odor elicits activity in more than one glomerulus. There are at least three glomeruli which show relatively high activity values during the time course of the simulation

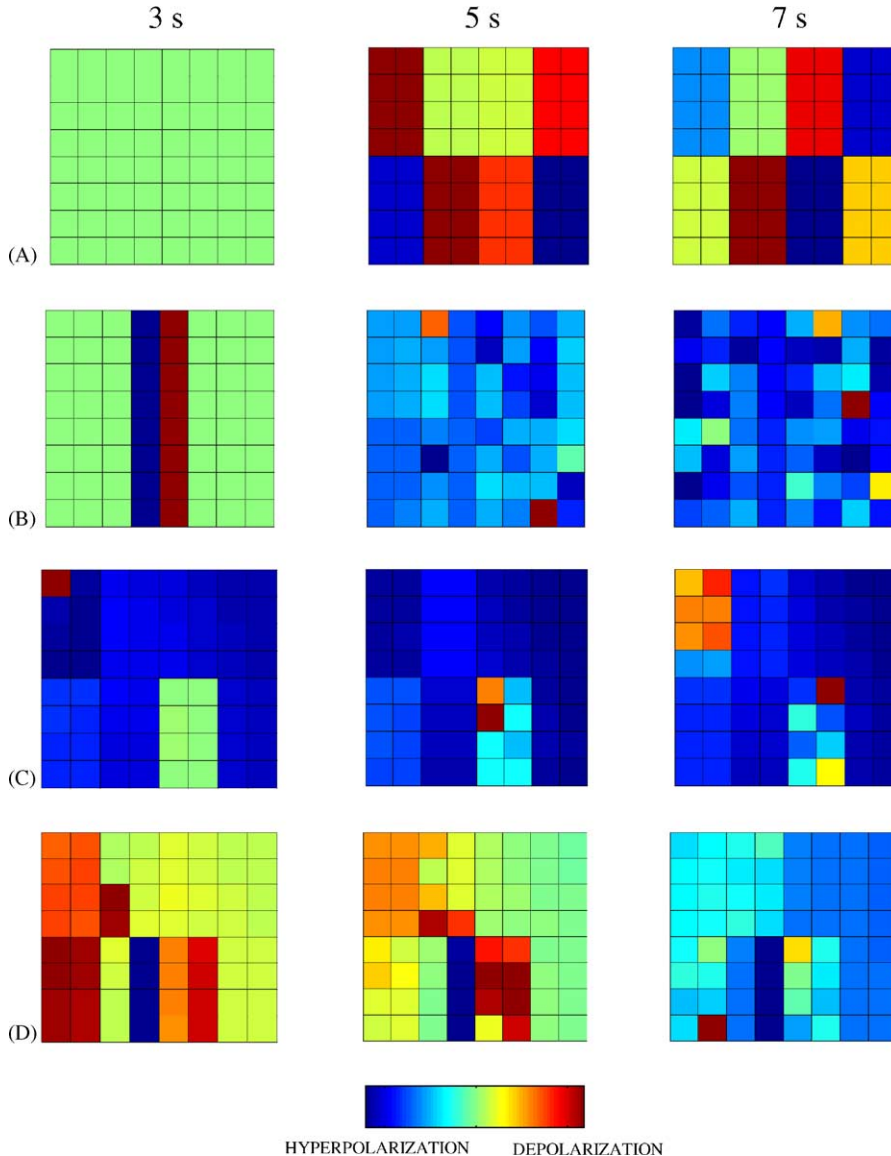


Fig. 7. Activity maps in the mitral cell layer of the model olfactory bulb for the instants 3 s (left column), 5 s (middle column) and 7 s (right column) after the presentation of  $300\ \mu\text{M}$  of the odor acetophenone. All gap junctions for this figure had coupling strength of  $300\ \text{M}\Omega$ . (A) Gap junctions in the olfactory epithelium, and blocked gap junctions and dendrodendritic synapses in the olfactory bulb. (B) Gap junctions in the olfactory epithelium and dendrodendritic synapses in the olfactory bulb, and blocked gap junctions in the olfactory bulb. (C) Gap junctions in the olfactory bulb, and gap junctions in the olfactory epithelium and dendrodendritic synapses in the olfactory bulb blocked. (D) Gap junctions and dendrodendritic synapses in the olfactory bulb, and gap junctions in the olfactory epithelium blocked. The color code used is the same of Fig. 2.

(counting glomeruli from top to bottom and from left to right, these are the second, the fifth and the seventh glomeruli). The activity pattern in the granule cell layer (Fig. 6, first row) again follows the activity pattern in the mitral cell layer, with a more or less diagonal area of activity going from the top left to the bottom right of the granule layer. This is due to the dendrodendritic synapses between mitral and granule cells. In the weak gap junction coupling case (Figs. 5 and 6, second row) the spatiotemporal patterns in the mitral and granule cell layers are even more distributed than in the same cases without dendrodendritic synapses. This trend can be observed for the intermediate values of gap junction coupling strength as well (Figs. 5 and 6, third and fourth rows). In the granule cell layer, the patterns with four active granule cells around a single active mitral cell vanish and a more irregular granule cell activity pattern can be observed. In the strong gap junction coupling strength regime, the behavior exhibited by the mitral and granule cell layers is similar to the one of the case without dendrodendritic synapses.

The results obtained in Cases 4, 5, 6, and 7 are shown in Fig. 7. This figure shows the activity maps in the mitral cell layer at three different time instants for the four cases considered. Fig. 7A shows the behavior for a gap junction coupling strength of  $300\text{ M}\Omega$  in the epithelium and no gap junctions and dendrodendritic synapses in the bulb. The glomeruli shapes are much easier to see in this case, and all of them participate in the odor representation in a way that is driven by the spatiotemporal activity pattern disseminated over the epithelium (see Fig. 2, fourth row). In Case 5, when dendrodendritic synapses are added to the bulb (Fig. 7B), the activity patterns become much more irregular and it is no longer possible to spot a single glomerulus. The results for Case 6 are shown in Fig. 7C. In this case the activity pattern in the epithelium consists of the red dots seen in the first row of Fig. 2, containing the OSNMs that project to the acetophenone glomerulus and other OSNMs that project to different glomeruli. The corresponding pattern in the mitral cell layer clearly shows the acetophenone glomerulus active over the whole duration of the simulation plus another glomerulus, the first one counting from top to bottom and left to right. Comparing this figure with the first row of Fig. 3, which gives a similar situation but with gap junctions blocked in the bulb, one can see that the introduction of the bulbar

gap junctions produced an alteration in the mitral layer response pattern. In the two cases the odor representation pattern is made of a combination of glomeruli (instead of single MNMs as in other cases) but the recruited glomeruli change from the case with bulbar gap junctions blocked to the case with bulbar gap junctions unblocked. The final case, shown Fig. 7D, is similar to the above but it contains dendrodendritic synapses in the bulb. The inclusion of the dendrodendritic synapses led to the appearance of a more irregular and widespread activity pattern in the mitral layer.

#### 4. Discussion

Neural oscillations triggered by odorant stimulation have often been reported at various levels of the olfactory nervous system in a wide variety of vertebrates (Adrian, 1957; Ottoson, 1959; Takagi and Shibuya, 1960; Sutterlin and Sutterlin, 1971; Hamilton and Kauer, 1989) and recent studies have addressed their role in odorant information coding (Laurent, 1999; Dorries and Kauer, 2000; Lam et al., 2000; Bokil et al., 2001; Friedrich and Stopfer, 2001; Laurent et al., 2001; Friedrich, 2002; Spors and Grinvald, 2002; Suzuki et al., 2002; Wachowiak et al., 2002). Dorries and Kauer (2000) have shown in the salamander the existence of odor-evoked oscillations in the olfactory epithelium and bulb. Their results suggest that the oscillations both in the olfactory epithelium and bulb have a common source and, by sectioning the olfactory nerve and injecting tetrodotoxin to the epithelium, they gathered evidence in favor of a peripheral source for the epithelium oscillations related to OSN spiking. The observed oscillations probably emerge from some sort of OSN communication, and gap junctions constitute one of the possible means of implementing this (Dorries and Kauer, 2000).

Several models in literature have been proposed to explain the origin of oscillations in the olfactory bulb (Rall and Shepherd, 1968; Freeman, 1975; Li and Hopfield, 1989; Meredith, 1992; White et al., 1992; Rospars and Fort, 1994; Linster and Hasselmo, 1997; Hendin et al., 1998; White and Kauer, 1999, 2001; Li and Hertz, 2000; Davison et al., 2001; Freeman et al., 2001; Laurent et al., 2001). However, little has been done to explain the origin of the peripheral voltage oscillations observed in the olfactory epithelium.

A recent computational model of current flow through the extracellular space between unmyelinated axons in the olfactory nerve (Bokil et al., 2001) showed that significant ephaptic interactions may occur for a range of physiologically relevant parameters, with an action potential in a single axon evoking action potentials in all other axons in the fascicle. This model showed that ephaptic interactions also can lead to synchronized firing of independently stimulated axons. Another recent computational model based the origin of neural oscillations triggered by odorant stimulation on the cAMP olfactory transduction signaling pathways of the OSN (Suzuki et al., 2002). The present study is one of the first to explore the possible effects of gap junction coupling on the initial stages of the olfactory system (Zhang et al., 2000; Zhang and Restrepo, 2002).

The constructed model of olfactory epithelium can be seen as an animation of the group of 162 cells described by Ma and Shepherd (2000) embedded in a grid of receptor cells, allowing the simultaneous visualization of the voltage values of a large number of OSNMs during odor stimulations. The model shows that the existence of gap junctions connecting OSNs in the olfactory epithelium are responsible for the generation of activity waves which propagate across the epithelium. Moreover, depending on the gap junction coupling strength these waves exhibit different behaviors. For weak gap junction coupling they are like thin spiral filaments, and for stronger coupling their spiral branches become wider and wave break happens leading to a situation in which most of the OSNMs are active during the time of odor presentation. This can be seen in Fig. 2 (first row) and in Fig. 8, which shows the percentage of active cells in the olfactory epithelium during odor stimulation.

To obtain the graphs in Fig. 8, we maintained the olfactory epithelium gap junction coupling strength at a constant value which causes wave propagation and wave break ( $R_{\text{gap}} = 300 \text{ M}\Omega$ ) and stimulate the olfactory epithelium with one of the eight different odors at a time. Fig. 8 shows that for all odors, there is a high percentage of OSNMs active during the entire duration of odor presentation. In particular, notice that for the odor acetophenone Fig. 8 shows that before the fourth second after the odor presentation the percentage of OSNMs that are active is relatively small (less than 20%) but after this time the percentage grows to

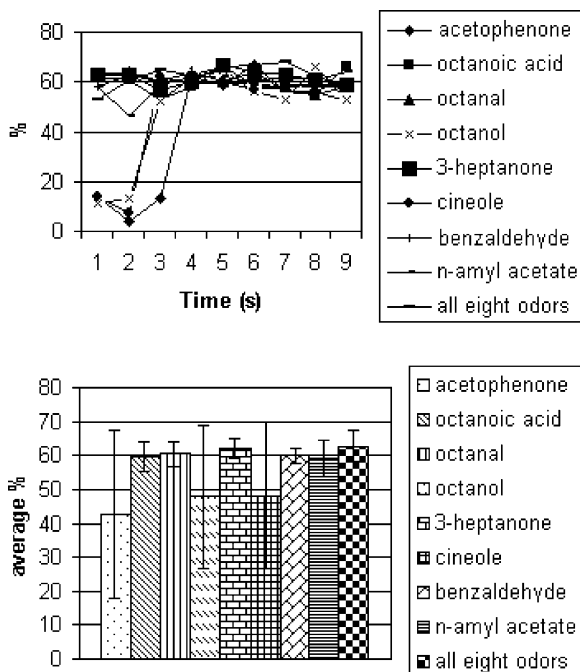


Fig. 8. (A) Percentage of active OSN cells as a function of the time after the presentation of  $300 \mu\text{M}$  of each one of the eight simulated odors. Whenever the membrane voltage of an OSN became higher than  $-35 \text{ mV}$  (the resting potential of an OSN is  $-55 \text{ mV}$ ) we considered that it was active. In all cases there are gap junction couplings in the olfactory epithelium with strength of  $300 \text{ M}\Omega$ . (B) Average (calculated between 1 and 9 s) percentage of active cells in the olfactory epithelium during the presentation of each one of the eight odors simulated. The average values are:  $59.33 \pm 5.32\%$  (*n*-amyl acetate),  $60 \pm 2.12\%$  (benzaldehyde),  $48.22 \pm 21.51\%$  (cineole),  $61.89 \pm 2.98\%$  (3-heptanone),  $47.89 \pm 21.02\%$  (octanol),  $60.44 \pm 3.54$  (octanal),  $59.67 \pm 4.53$  (octanoic acid),  $42.56 \pm 24.68\%$  (acetophenone). The average value when all the eight odors were presented simultaneously was  $60.67 \pm 4.66\%$ .

around 60% and remains there. The graphs shown in Fig. 2 are all for times after 5 s, so that they apply for the case of high percentage of active OSNMs. Since the average activity level remains more or less constant around 60%, this suggests that the wave propagation and annihilation due to gap junction coupling in the olfactory epithelium generates a self-organizing mechanism that constantly tunes this system to a high degree of activity. This might be a source of synchronous activity in the olfactory epithelium.

Gap junction coupling in the olfactory epithelium suggests a new mechanism of odor coding by the olfactory system, due to wave interaction, which is

complementary to the one based on overlapping organization of afferents into glomeruli (Malnic et al., 1999; Laurent et al., 2001). The results of the simulations have shown that the existence of gap junctions of varying coupling strengths in the olfactory epithelium causes different spatiotemporal activity patterns in the olfactory bulb which are, in turn, different from the patterns existing when the gap junctions in the olfactory epithelium are blocked. This suggests that if functional gap junctions are proven to exist in the olfactory epithelium the spatiotemporal odor representation found in the olfactory bulb might be driven by a spatiotemporal odor representation in the olfactory epithelium. In other words, odor coding might start already at the odor receptor layer.

A problem with the view that olfactory epithelium odor-evoked wave-like patterns may code odors is that the propagation of the waves generated at OSN clusters across the whole epithelium causes an overlap of the receptive ranges of different OSNs, thus decreasing the system's specificity. Using information theory analysis (Alkasab et al., 1999) and a generalized framework for modeling odorants and olfactory receptors, Alkasab et al. (2002) have shown that sensors with a substantial overlap of their receptive ranges carry redundant information. Less obviously, they also have shown that sensors whose receptive ranges do not overlap at all have greater information redundancy than sensors whose receptive ranges partially overlap (Alkasab et al., 2002). Therefore, the receptive range overlap provoked by the propagating waves might not be a totally undesirable effect, if properly tuned.

The mechanism of wave propagation and annihilation in the olfactory epithelium might be a self-organizing mechanism that tunes the receptive ranges of the receptor cells to a partially overlapped state. This mechanism could improve the performance of the sensory network to allow the capture of the largest amount of information possible about different stimuli and, at the same time, protecting it from an over-activation. Moreover, since the positions of OSNs in the epithelium are constantly being modified because of OSN turnover (Graziadei and Graziadei, 1979) this self-organizing mechanism might provide a way of continually retuning the receptive system in order to keep it capable of capturing information about odors and their concentrations in a stable way amidst its changing environment.

In this work, we have studied several different possibilities of combining gap junctions with varying coupling strengths in the olfactory epithelium and in the olfactory bulb, and of combining these with dendrodendritic synapses in the olfactory bulb. The results showed distributed spatiotemporal patterns produced in the olfactory bulb model during odor stimulation, with several glomeruli activated by a single odorant and a widely distributed response over time involving many glomeruli. These results are qualitatively similar to recent experimental findings (Spors and Grinvald, 2002) and are compatible with the possibility of a combinatorial code in the olfactory epithelium and olfactory bulb, with a given odor activating different OSNs and glomeruli at different instants in time, and a given glomerulus and OSN being activated by different odors (Cinelli et al., 1995; Bozza and Kauer, 1998; Friedrich and Korsching, 1998; Malnic et al., 1999; Rubin and Katz, 1999; Lam et al., 2000; Ma and Shepherd, 2000; Uchida et al., 2000; Belluscio and Katz, 2001; Bozza and Mombaerts, 2001; Meister and Bonhoeffer, 2001; Wachowiak and Cohen, 2001; Fried et al., 2002; Spors and Grinvald, 2002; Wachowiak et al., 2002).

It is possible that some of the mechanisms described in the present work may exist in other brain systems where there are neurons connected by gap junctions (Condorelli et al., 2000; Rozental et al., 2000). In particular, these mechanisms could be present in the generation of spatiotemporal wave-like patterns observed in the retina (Roerig and Feller, 2000; Deans et al., 2002).

## 5. Conclusion

This work has shown that the spatiotemporal activity patterns in the olfactory bulb could be, at least partially, a consequence of propagating activity waves in the olfactory epithelium with OSNs connected via gap junctions. A suggestion that comes from this result is that odor coding might start already at the olfactory epithelium or, at least, that the olfactory epithelium is not a passive receptor layer but processes odor information as well. A possible role for the existence of gap junctions in the olfactory epithelium and olfactory bulb, as well as of the existence of the dendrodendritic synapses in the olfactory bulb, would

be to distribute the odor-evoked activity over the epithelium and bulb, thus broadly tuning these systems (Reyher et al., 1991; Trotier, 1998; Condorelli et al., 2000; Zhang et al., 2000; Zhang and Restrepo, 2002).

The constructed model or improved versions of it may be used as tools for testing different hypotheses and scenarios related to information processing and coding in the olfactory system.

## Acknowledgements

Research supported by FAPESP.

## Appendix A

The single cell parameters listed in this appendix are:  $C_m$ : membrane capacitance ( $F/m^2$ );  $R_m$ : membrane resistance ( $\Omega m^2$ );  $R_a$ : axial resistance ( $\Omega m$ );  $V_{rep}$ : rest potential (V);  $D_x$ : diameter of a compartment  $x$  ( $\mu m$ ); and  $L_x$ : length of a compartment  $x$  ( $\mu m$ ). We give below these values for the OSNM, the MNM, and the GNM.

- *OSNM*:  $C_m = 0.01$ ;  $R_m = 11$ ;  $R_a = 1$ ;  $V_{rep} = -0.055$ ;  $D_{soma} = 10$ ;  $L_{soma} = 13$ ;  $D_{dendrite} = 2$ ;  $L_{dendrite} = 70$ ;  $D_{dendritic\_knob} = 3$ ;  $L_{dendritic\_knob} = 3$ . Threshold:  $V = -0.035$  V. The somatic ionic channels and densities Traub et al. (1991). The simulated calcium dependent chloride channel of the dendritic knob has a maximum conductance of 3 ns and an equilibrium potential of +6 mV (Reuter et al., 1998). The details about this channel can be found at <http://www.genesis-sim.org/BABEL/babeldirs/models/C1chan/>.
- *MNM*:  $C_m = 0.01$ ;  $R_m = 10$ ;  $R_a = 2$ ;  $V_{rep} = -0.065$ ;  $D_{soma} = 32$ ;  $L_{soma} = 32$ ;  $D_{primary\_dendrite} = 7.9$ ;  $L_{primary\_dendrite} = 370$ ;  $D_{secondary\_dendrite} = 5.8$ ;  $L_{secondary\_dendrite} = 500$ ;  $D_{tuft} = 3.5$ ;  $L_{tuft} = 180$ . The simulated channels and densities are the same of Bhalla and Bower (1993). Threshold:  $V = -0.03$  V.
- *GNM*:  $C_m = 0.01$ ;  $R_m = 12$ ;  $R_a = 0.5$ ;  $V_{rep} = -0.065$ ;  $D_{soma} = 6$ ;  $L_{soma} = 8$ ;  $D_{periphic\_dendrite} = 1.25$ ;  $L_{periphic\_dendrite} = 200$ ;  $D_{deep\_dendrite} = 1$ ;  $L_{deep\_dendrite} = 100$ ;  $D_{trunk} = 2$ ;  $L_{trunk} = 200$ ;  $D_{spine\_head} = 1$ ;  $L_{spine\_head} = 3$ ;  $D_{spine\_neck} = 0.2$ ;

$L_{spine\_neck} = 1$ . The simulated channels and densities are the same of Bhalla and Bower (1993). Threshold:  $V = -0.03$  V.

More details about the construction and validation of the simulated cells, as well as about the whole model of the olfactory system used in this work can be found in Simões-de-Souza's M.Sc. thesis (in Portuguese), which is available at <http://www.teses.usp.br/teses/disponiveis/59/59134/tde-14092002-092930/>.

## References

- Adrian, E.D., 1957. Potential oscillations in the olfactory organ. *J. Physiol. Lond.* 128, 21–22.
- Alkasab, T.K., Bozza, T.C., Cleland, T.A., Dorries, K.M., Pearce, T.C., White, J., Kauer, J.S., 1999. Characterizing complex chemosensors: information-theoretic analysis of olfactory system. *Trends Neurosci.* 22, 102–108.
- Alkasab, T.K., White, J., Kauer, J.S., 2002. A computational system for simulating and analyzing arrays of biological and artificial chemical sensors. *Chem. Senses* 27, 261–275.
- Belluscio, L., Katz, L.C., 2001. Symmetry, stereotypy, and topography of odorant representation in mouse olfactory bulbs. *J. Neurosci.* 21, 2113–2122.
- Bhalla, U.S., Bower, J.M., 1993. Exploring parameter space in detailed single neuron models: simulations of the mitral and granule cells of the olfactory bulb. *J. Neurophysiol.* 69, 1948–1965.
- Bokil, H., Laaris, N., Blinder, K., Ennis, M., Keller, A., 2001. Ephaptic interactions in the mammalian olfactory system. *J. Neurosci.* 21 (1–5), RC173.
- Bower, J.M., Beeman, D., 1998. *The Book of GENESIS: Exploring Realistic Neural Models with the General Neural Simulation System*, 2nd ed. TELOS, Santa Clara.
- Bozza, T.C., Kauer, J.S., 1998. Odorant response properties of convergent olfactory receptor neurons. *J. Neurosci.* 18, 4560–4569.
- Bozza, T.C., Mombaerts, P., 2001. Olfactory coding: revealing intrinsic representations of odors. *Curr. Biol.* 11, R687–R690.
- Brennan, P.A., Keverne, E.B., 1997. Neural mechanisms of mammalian olfactory learning. *Prog. Neurobiol.* 51, 457–481.
- Cinelli, A.R., Hamilton, K.A., Kauer, J.S., 1995. Salamander olfactory bulb neural activity observed by video rate, voltage-sensitive dye imagines III. Spatial and temporal properties of responses evoked by odorant stimulation. *J. Neurophysiol.* 73, 2053–2071.
- Condorelli, D.F., Belluardo, N., Trovato-Salinaro, A., Mudd, G., 2000. Expression of Cx36 in mammalian neurons. *Brain Res. Rev.* 32, 72–85.
- Davison, A.P., Feng, J., Brown, D., 2001. Spike synchronization in a biophysically-detailed model of the olfactory bulb. *Neurocomputing* 38–40, 515–521.

- De Schutter, E., Smolen, P., 1998. Calcium dynamics in large neuronal models. In: *Methods in Neural Modeling: From Ions to Networks*, 2nd ed. MIT Press, Cambridge, Chapter 6, pp. 211–250.
- Deans, M.R., Volgyi, B., Goodenough, D.A., Bloomfield, S.A., Paul, D.L., 2002. Connexin 36 is essential for transmission of rod-mediated visual signals in the mammalian retina. *Neuron* 36, 703–712.
- Desmaisons, D., Vicent, J.-D., Ledo, P.-M., 1999. Control of action potential timing by intrinsic subthreshold oscillations in olfactory bulb output neurons. *J. Neurosci.* 15, 10727–10737.
- Didier, A., Carleton, A., Bjaalie, J.G., Vicent, J.-D., Ottersen, O.P., Storm-Mathisen, J., Lledo, P.-M., 2001. A dendrodendritic reciprocal synapse provides a recurrent excitatory connection in the olfactory bulb. *Proc. Natl. Acad. Sci. U.S.A.* 98, 6441–6446.
- Dorries, K.M., Kauer, J.S., 2000. Relationships between odor-elicited oscillations in the salamander olfactory epithelium and olfactory bulb. *J. Neurophysiol.* 83, 754–765.
- Duchamp, A., Reval, M.F., Holley, A., MacLeod, P., 1974. Odor discrimination by frog olfactory neurons. *Chem. Senses* 1, 213–233.
- Duchamp-Viret, P., Chaput, M.A., Duchamp, A., 1999. Odor response properties of rat olfactory receptor neurons. *Science* 284, 2171–2174.
- Èrdi, P., Aradi, I., Kato, Y., Yoshikawa, K., 1998. Dynamic information processing in natural and artificial olfactory systems. *Biosystems* 46, 107–112.
- Firestein, S., Picco, C., Menini, A., 1993. The relation between stimulus and response in olfactory receptor cells of the tiger salamander. *J. Physiol.* 463, 1–10.
- Freeman, W.J. (Ed.), 1975. *Mass Action in the Nervous System*. Academic Press, New York.
- Freeman, W.J., Kozma, R., Werbos, P.J., 2001. Biocomplexity: adaptive behavior in complex stochastic dynamical systems. *Biosystems* 59, 109–123.
- Fried, H.S., Fuss, S.H., Korsching, S.I., 2002. Selective imaging of presynaptic activity in the mouse olfactory bulb shows concentration and structure dependence of odor responses in identified glomeruli. *Proc. Natl. Acad. Sci. U.S.A.* 99, 3222–3227.
- Friedman, D., Strowbridge, B.W., 2000. Functional role of NMDA autoreceptors in olfactory mitral cells. *J. Neurophysiol.* 84, 39–50.
- Friedrich, R.W., 2002. Real time odor representations. *Trends Neurosci.* 25, 487–489.
- Friedrich, R.W., Korsching, S.I., 1998. Chemotopic, combinatorial, and noncombinatorial odorant representations in the olfactory bulb revealed using a voltage-sensitive axon tracer. *J. Neurosci.* 18, 9977–9988.
- Friedrich, R.W., Stopfer, M., 2001. Recent dynamics in olfactory population coding. *Curr. Opin. Neurobiol.* 11, 468–474.
- Gesteland, R.C., Lettvin, J.Y., Pitts, W.H., 1965. Chemical transmission in the nose of the frog. *J. Physiol. Lond.* 181, 525–559.
- Getchell, T.V., 1974. Unitary responses in frog olfactory epithelium to sterically related molecules at low concentration. *J. Gen. Physiol.* 64, 241–261.
- Graziadei, P.P., Graziadei, G.A., 1979. Neurogenesis and neuron regeneration in the olfactory system of mammals. I. Morphological aspects of differentiation and structural organization of the olfactory sensory neurons. *J. Neurocytol.* 8, 1–18.
- Halabisky, B., Friedman, D., Radojicic, M., Strowbridge, B.W., 2000. Calcium influx through NMDA receptors directly evokes GABA release in olfactory bulb granule cells. *J. Neurosci.* 20, 5124–5134.
- Hallani, M., Lynch, J.W., Barry, P.H., 1998. Characterization of calcium-activated chloride channels in patches excised from dendritic knob of mammalian olfactory receptor neurons. *J. Member. Biol.* 161, 163–171.
- Hamilton, K.A., Kauer, J.S., 1989. Patterns in intracellular potentials in salamander mitral/ruft cells in response to odor stimulation. *J. Neurophysiol.* 59, 609–625.
- Hendin, O., Horn, D., Tsodyks, M.V., 1998. Associative memory and segmentation in an oscillatory neural model of the olfactory bulb. *J. Comput. Neurosci.* 5, 157–169.
- Henriquez, A.P., Vogel, R., Muller-Borer, B.J., Henriquez, C.S., Weingart, R., Cascio, W.E., 2001. Influence of dynamic gap junction resistance on impulse propagation in ventricular myocardium: a computer simulation study. *Biophys. J.* 81, 2112–2121.
- Heyward, P., Ennis, M., Keller, A., Shipley, M.T., 2001. Membrane bistability in olfactory bulb mitral cells. *J. Neurosci.* 21, 5311–5320.
- Hirono, J., Sato, T., Tonoike, M., Takebayashi, M., 1994. Local distribution of odor responsiveness of mouse olfactory receptor neurons. *Neurosci. Lett.* 174, 201–204.
- Isaacson, J.S., 1999. Glutamate spillover mediates excitatory transmission in the rat olfactory bulb. *Neuron* 23, 377–384.
- Isaacson, J.S., 2001. Mechanisms governing dendritic  $\lambda$ -aminobutyric acid (GABA) release in the rat olfactory bulb. *Proc. Natl. Acad. Sci. U.S.A.* 98, 337–342.
- Kashiwadani, H., Sasaki, Y.F., Uchida, N., Mori, K., 1999. Synchronized oscillatory discharges of mitral/tufted cells with different molecular receptive ranges in the rabbit olfactory bulb. *J. Neurophysiol.* 82, 1786–1792.
- Kauer, J.S., White, J., 2001. Imaging and coding in the olfactory system. *Annu. Rev. Neurosci.* 24, 963–979.
- Korsching, S., 2002. Olfactory maps and odor images. *Curr. Opin. Neurobiol.* 12, 387–392.
- Kurahashi, T., Yau, K.-W., 1994. Tale of an unusual chloride current. *Curr. Biol.* 4, 256–258.
- Lam, Y.-W., Cohen, L.B., Wachowlak, M., Zochowski, M.R., 2000. Odors elicit three different oscillations in the turtle olfactory bulb. *J. Neurosci.* 20, 749–762.
- Laurent, G., 1999. A systems perspective on early olfactory coding. *Science* 286, 723–728.
- Laurent, G., Stopfer, M., Friedrich, R.W., Rabinovich, M.I., Volkovskii, A., Abarbanel, H.D.I., 2001. Odor encoding as an active, dynamical process: experiments, computation and theory. *Annu. Rev. Neurosci.* 24, 263–297.
- Li, Z., Hertz, J., 2000. Odour recognition and segmentation by a model olfactory bulb and cortex. *Network* 11, 83–102.
- Li, Z., Hopfield, J.J., 1989. Modeling the olfactory bulb and its neural oscillatory processing. *Biol. Cybern.* 61, 379–392.

- Linster, C., Hasselmo, M., 1997. Modulation of inhibition in a model of olfactory bulb reduces overlap in the neural representation of olfactory stimuli. *Behav. Brain Res.* 84, 117–127.
- Lowe, G., Gold, H., 1993. Nonlinear amplification by calcium-dependent chloride channels in olfactory receptor cells. *Nature* 366, 283–286.
- Ma, M., Shepherd, G.M., 2000. Functional mosaic organization of mouse olfactory receptor neurons. *Proc. Natl. Acad. Sci. U.S.A.* 97, 12869–12874.
- Malnic, B., Hirono, J., Sato, T., Buck, L.B., 1999. Combinatorial receptor codes for odors. *Cell* 96, 713–723.
- McQuiston, A.R., Katz, L.C., 2001. Electrophysiology of interneurons in the glomerular layer of the rat olfactory bulb. *J. Neurophysiol.* 86, 1899–1907.
- Meister, M., Bonhoeffer, T., 2001. Tuning and topography in an odor map on the rat olfactory bulb. *J. Neurosci.* 21, 1351–1360.
- Menini, A., 1999. Calcium signaling and regulation in olfactory neurons. *Curr. Opin. Neurobiol.* 9, 419–426.
- Meredith, M., 1992. Neural circuit computation: complex patterns in the olfactory bulb. *Brain Res. Bull.* 29, 111–117.
- Mombaerts, P., 1996. Targeting olfaction. *Curr. Opin. Neurobiol.* 6, 481–486.
- Mombaerts, O., Wang, F., Dulac, C., Chao, S.K., Nemes, A., Mendelshon, M., Edmondson, J., Axel, R., 1996. Visualizing an olfactory sensory map. *Cell* 87, 675–686.
- Morri, K., Mataga, N., Imamura, K., 1992. Differential specificities of single mitral cells in rabbit olfactory bulb for a homologous series of fatty acid odor molecules. *J. Neurophysiol.* 67, 786–789.
- Morri, K., Nagao, H., Sasaki, Y.F., 1998. Computation of molecular information in mammalian olfactory system. *Network* 9, R79–R102.
- Morrison, E.E., Constanzo, R.M., 1990. Morphology of the human olfactory epithelium. *J. Comp. Neurol.* 297, 1–13.
- Ottoson, D., 1959. Studies on slow potentials in the rabbit's olfactory bulb and nasal mucosa. *Acta Physiol. Scand.* 47, 136–148.
- Pearce, T.C., 1997. Computational parallels between the biological olfactory pathway and its analogue 'The electronic Nose': Part I. *Biol. Olfaction Biosyst.* 41, 43–67.
- Rall, W., Shepherd, G.M., 1968. Theoretical reconstruction of field potentials and dendrodendritic synapses interactions in olfactory bulb. *J. Neurophysiol.* 31, 884–915.
- Ressler, K.J., Sullivan, S.L., Buck, L., 1993. A zonal organization of odorant receptor gene expression in the olfactory epithelium. *Cell* 73, 597–609.
- Ressler, K.J., Sullivan, S.L., Buck, L., 1994. Information coding in the olfactory system: evidence for a stereotyped and highly organized epitope map in the olfactory bulb. *Cell* 79, 1245–1255.
- Reuter, D., Zierold, K., Schroder, W.H., Frings, S., 1998. A depolarizing chloride current contributes to chemoelectrical transduction in olfactory sensory neurons in situ. *J. Neurosci.* 18, 6623–6630.
- Revial, M.F., Duchamp, A., Holley, A., 1978. Odour discrimination by frog olfactory receptors: a second study. *Chem. Senses* 3, 7–21.
- Reyher, C.K.H., Lübke, J., Larsen, W.J., Hendrix, G.M., Shipley, M.T., Baumgarten, M.G., 1991. Olfactory bulb granule cell aggregates: morphological evidence for interperikaryal electrotonic coupling via gap junctions. *J. Neurosci.* 11, 1485–1495.
- Roerig, B., Feller, M.B., 2000. Neurotransmitters and gap junctions in developing neural circuits. *Brain Res. Rev.* 32, 86–114.
- Rospars, J.-P., Fort, J.-C., 1994. Coding of odour quality: roles of convergence and inhibition. *Network* 5, 121–145.
- Rozental, R., Giaume, C., Spray, D.C., 2000. Gap junctions in the nervous system. *Brain Res. Rev.* 32, 11–15.
- Rubin, B.D., Katz, L.C., 1999. Optical imaging of odorant representations in the mammalian olfactory bulb. *Neuron* 23, 499–511.
- Sato, T., Hirono, J., Tonoike, M., Takebayashi, M., 1994. Tuning specificities to aliphatic odorants in mouse olfactory receptor neurons and their local distribution. *J. Neurophysiol.* 72, 2980–2989.
- Schild, R., Restrepo, D., 1998. Transduction mechanisms in vertebrate olfactory receptor cells. *Physiol. Rev.* 78, 429–466.
- Schoppa, N.E., Westbrook, G.L., 2001. Glomerulus-specific synchronization of mitral cells in the olfactory bulb. *Neuron* 21, 639–651.
- Schoppa, N.E., Kinzie, J.M., Sahara, Y., Segerson, T.P., Westbrook, G.L., 1998. Dendrodendritic inhibition in the olfactory bulb is driven by NMDA receptors. *J. Neurosci.* 18, 6790–6802.
- Simões-de-Souza, F.M., Roque, C., 2002. Simulation of a vertebrate receptor cell of the olfactory epithelium for use in network models. *Neurocomputing* 44–46, 177–182.
- Spors, H., Grinvald, A., 2002. Spatio-temporal dynamics of odor representations in the mammalian olfactory bulb. *Neuron* 34, 301–315.
- Sutterlin, A.M., Sutterlin, N., 1971. Electrical responses of the olfactory epithelium of *Atlantic salmon (Salmo salar)*. *J. Fish. Res. Bd. Can.* 28, 565–572.
- Suzuki, N., Takahata, M., Sato, K., 2002. Oscillatory current responses of olfactory receptor neurons to odorants and computer simulation based on a cyclic AMP transduction model. *Chem. Senses* 27, 789–801.
- Takagi, S.F., Shibuya, T., 1960. Potential oscillations in the lower olfactory pathway of the toad. *Nature* 186, 724.
- Traub, R.D., Wong, R.K., Miles, R., Michelson, H., 1991. A model of a CA3 hippocampal pyramidal neuron incorporating voltage-clamp data on intrinsic conductances. *J. Neurophysiol.* 66, 635–650.
- Traub, R.D., Schmitz, D., Jefferys, J.G.R., Draguhn, A., 1999. High-frequency population oscillations are predicted to occur in hippocampal pyramidal networks interconnected by axoaxonal gap junctions. *Neuroscience* 92, 407–426.
- Trotier, D., 1998. Electrophysiological properties of frog olfactory supporting cells. *Chem. Senses* 23, 363–369.
- Trotier, D., MacLeod, P., 1983. Intracellular recordings from salamander olfactory receptor cells. *Brain Res.* 268, 225–237.
- Uchida, N., Takahashi, Y.K., Tanifuji, M., Mori, K., 2000. Odor maps in the mammalian olfactory bulb: domain organization and odorant structural features. *Nat. Neurosci.* 3, 1035–1043.
- Urban, N.N., Sakmann, B., 2002. Reciprocal intraglomerular excitation and intra- and interglomerular lateral inhibition

- between mouse olfactory bulb mitral cells. *J. Physiol.* 542.2, 335–367.
- Vassar, R., Ngai, J., Axel, R., 1993. Spatial segregation of odorant receptor expression in the mammalian olfactory epithelium. *Cell* 74, 309–318.
- Vassar, R., Chao, S., Sitchan, R., Nunez, J., Vosshall, L., Axel, R., 1994. Topographic organization of sensory projections to the olfactory bulb. *Cell* 79, 981–991.
- Yokoi, M., Mori, K., Kananishi, S., 1995. Refinement of odor molecule tuning by dendrodendritic synaptic inhibition in the olfactory bulb. *Proc. Natl. Acad. Sci. U.S.A.* 92, 3371–3375.
- Wachowiak, M., Cohen, L.B., 2001. Representation of odorants by receptor neuron input to the mouse olfactory bulb. *Neuron* 32, 723–735.
- Wachowiak, M., Cohen, L.B., Zochowski, M.R., 2002. Distributed and concentration-invariant spatial representations of odorants by receptor neuron input to the turtle olfactory bulb. *J. Neurophysiol.* 87, 1035–1045.
- Wellis, D.P., Scott, J.W., Harrison, T.A., 1989. Discrimination among odorants by single neurons of the rat olfactory bulb. *J. Neurophysiol.* 61, 1161–1177.
- White, J., Kauer, J.S., 1999. Odor recognition in an artificial nose by spatio-temporal processing using an olfactory neural network. *Neurocomputing* 26/27, 919–924.
- White, J., Kauer, J.S., 2001. Exploring olfactory population coding using an artificial olfactory system. *Prog. Brain Res.* 130, 191–203.
- White, J., Hamilton, K.A., Neff, S.R., Kauer, J.S., 1992. Emergent properties of odor information coding in a representational model of the salamander olfactory bulb. *J. Neurosci.* 12, 1772–1780.
- Woolf, T.B., Shepherd, G.M., Greer, C.A., 1991. Local information processing in dendritic trees: subsets of spines in granule cells of the mammalian olfactory bulb. *J. Neurosci.* 11, 1837–1854.
- Zador, A., Kock, C., Brown, T.H., 1990. Biophysical model of a Hebbian synapse. *Proc. Natl. Acad. Sci. U.S.A.* 87, 6718–6722.
- Zhang, C., Restrepo, D., 2002. Expression of connexin 45 in the olfactory system. *Brain Res.* 929, 37–47.
- Zhang, C., Finger, E., Restrepo, D., 2000. Mature olfactory receptor neurons express connexin 43. *J. Comp. Neurol.* 426, 1–12.
- Zufall, F., Leinders-Zufall, T., 2000. The cellular and molecular basis of odor adaptation. *Chem. Senses* 25, 473–481.